



# Fracture Toughness Estimation From Ceramic Tensile Specimens by Fractographic Analysis

by R. Nathan Katz  
and Kyu Cho

ARL-TR-1405

June 1997

DTIC QUALITY INSPECTED 4

19970722 174

The findings in this report are not to be construed as an official Department of the Army position unless so designated by other authorized documents.

Citation of manufacturer's or trade names does not constitute an official endorsement or approval of the use thereof.

Destroy this report when it is no longer need. Do not return it to the originator.

# Army Research Laboratory

Aberdeen Proving Ground, MD 21005-5069

---

ARL-TR-1405

June 1997

---

## Fracture Toughness Estimation From Ceramic Tensile Specimens by Fractographic Analysis

R. Nathan Katz

Worcester Polytechnic Institute

Kyu Cho

Weapons and Materials Research Directorate, ARL

---

## Abstract

---

Empirical criteria are presented for selection of uniaxial tensile failure origins that will yield valid fracture toughness estimations. Using these criteria, estimations of fracture toughness based on fractography of an AlN, two SiCs, a AlN-SiC solid solution and a particulate composite, and a TiB<sub>2</sub> were performed. Comparison of the fracture toughness values estimated from fractography with fracture toughness measured by the single-edge precracked beam (SEPB) method will be shown. Close agreement is observed between estimates made from fractographic analysis and measurements made on specimens with large artificially induced flaws if the fracture toughness is 4 MPa√m or below. For materials in which the SEPB fracture toughness is greater than about 4.8 MPa√m, estimates by fractographic analysis significantly underestimate the SEPB fracture toughness. In attempting to rationalize this discrepancy, the importance of rigorously applying the empirical criteria was reemphasized.

# Table of Contents

	<u>Page</u>
<b>List of Figures</b> .....	v
<b>List of Tables</b> .....	v
<b>1. Introduction</b> .....	1
<b>2. Experimental Technique</b> .....	2
<b>3. Criteria for Estimation of <math>K_{IC}</math> by Fractographic Analysis</b> .....	5
<b>4. Estimation of <math>K_{IC}</math></b> .....	8
<b>5. Potential Sources of Discrepancy Between Estimated and Measured <math>K_{IC}</math> at "High" <math>K_{IC}</math></b> .....	11
<b>6. The Fracture Initiating Flaw vs. the Critical Flaw</b> .....	12
<b>7. Summary</b> .....	14
<b>8. References</b> .....	15
<b>Distribution List</b> .....	17
<b>Report Documentation Page</b> .....	21

INTENTIONALLY LEFT BLANK.

## List of Figures

<u>Figure</u>	<u>Page</u>
1. Hydraulic Pressure Chamber With Specimen-Piston Assembly .....	4
2. Circular Fracture Mirror in AlN .....	7
3. Elliptical Fracture Mirror in AlN-SiC Solid Solution Unacceptable for Analysis .	7
4. "Pseudo" Mirror in TiB <sub>2</sub> Shows Mist and Hackle But No Mirror .....	8
5. SiC Pad B Shows Mirror, Mist, and Hackle .....	9
6. SiC Pad N Shows Only Mist and Hackle .....	9
7. Fracture Toughness Comparison Between Fractographic Estimates and SEPB Measurements .....	10

## List of Tables

<u>Table</u>	<u>Page</u>
1. Materials and Property Data Used in This Study .....	5
2. Anticipated vs. Observed Flaw Size .....	11

INTENTIONALLY LEFT BLANK.



# 1. Introduction

Fractography is widely used to identify failure initiating flaws and flaw populations in advanced ceramics. However, fractography is seldom used to determine the fracture toughness of ceramics. This is surprising, since fractography has long been used to estimate the fracture energy of brittle materials, glasses in particular. One such study of the use of fractography to calculate fracture surface energy for a wide variety of ceramics and glasses was conducted by Mecholsky et al. [1]. They were able to show a good correlation between the size of the outer fracture mirror in bend specimens and  $K_{IC}$  as measured in a double cantilever beam (DCB) test. Rice [2] presented a comprehensive paper on the fractographic determination of  $K_{IC}$  in ceramics at the Second Conference on the Fractography of Glass and Ceramics in 1990. He showed that, for bend bars with large flaws, good agreement was obtained between  $K_{IC}$  estimated from fractographic analysis and DCB tests. However, as the flaw sizes decreased, there was a marked tendency for an increasing disparity between the fracture toughness or fracture energies estimated by fractographic analysis and DCB measurements.

In the past several years, two very useful documents [3, 4] have been prepared by researchers at the U.S. Army Research Laboratory (ARL) and the National Institute of Science and Technology, which provide handbook-type guidance in the use of fractography and the relationship between fractography and fracture toughness, but they provide no specific data correlating  $K_{IC}$  and fracture origins. Swab and Quinn [4] contains a very useful appendix, which discusses, in detail, various circumstances that might cause discrepancies in estimates of fracture origin size predictions from fracture mechanics, and fractographically observed flaw sizes. Virtually all examples of the use of fracture mechanics to estimate critical flaw sizes or fracture energies/toughness discussed in the previously listed references involved bend tests where fracture origins were often associated with surface machining damage.

With the growing use of tensile testing in the determination of strength statistics for advanced ceramics, a large number of samples of known uniaxial tensile stress and unambiguous failure

origins have become available for analysis. Little work has been reported on using fractography of uniaxial tensile test specimens to estimate fracture toughness. One early work that used fractography of carefully lapped uniaxial tensile specimens of HS130\* Si<sub>3</sub>N<sub>4</sub> (an early version of NC132\* material) [5] yielded an estimated  $K_{IC}$  of 2.8 MPa√m. No correlation with measured values was made. Recent work by Katz and his coworkers [6] compared  $K_{IC}$  estimated by fractographic analysis and those measured by a single-edge precracked beam test (SEPB) for an AlN, a 50%/50% AlN-SiC solid solution and a 25% SiC particulate toughened AlN composite. For all three materials, the agreement between estimated and measured  $K_{IC}$  values was within 10%. In a subsequent study of two SiC materials, it was observed that the SiC with a  $K_{IC}$  of 4.9 MPa√m showed the largest deviation (-12%) from measured SEPB values of any material that we had tested [7]. A study by Oishi et al. [8], conducted on Y-TZP material, also compared measured  $K_{IC}$  (by SEPB) with estimates from fractography. Fractographic estimates were as much as 35% less than the SEPB values.

The purpose of the work discussed in this report was to extend the range of polycrystalline ceramics for which estimates of  $K_{IC}$  could be compared to measured values. TiB<sub>2</sub>, which has a moderately high  $K_{IC}$  and a moderate tensile strength, was chosen as a material that would likely produce a reasonable percentage of internal, as opposed to machining induced, failure origins. Discrepancies between estimated and measured values for TiB<sub>2</sub> and other "high"  $K_{IC}$  ceramics are rationalized in terms of subcritical crack growth and/or R-curve behavior. Consideration of the consequences of subcritical crack growth reemphasizes the difference between the failure initiating flaw and the critical flaw, even though the later contains the former. Fractographs showing a hierarchy of concentric flaws in a TiB<sub>2</sub> specimen will be presented to emphasize this point.

## 2. Experimental Technique

The tensile specimens used in this work were right circular cylinders, measuring between 100 and 120 mm in length and 8.8–9.2 mm in diameter. 40 mm on each end of the test specimen were

---

\* Norton Co., Worcester, MA 01606.

inserted into a steel piston and adhesively bonded in place with high-strength epoxy\* [9–11]. The adhesively bonded specimen-piston assembly is inserted into the pressure chamber of an ASCERA Hydraulic Tensile Tester.† Pressure is applied via a hydraulic fluid and increased at a rate of approximately 3 MPa per second until the specimen is broken apart by the hydraulic pressure acting against the piston faces. Figure 1 shows a schematic of the pressure chamber with the adhesively bonded specimen-piston assembly in place. The tensile fracture stress is calculated using the pressure at the instant of failure and the geometric parameters of the specimen-piston assembly [9–11]. Although this tensile testing method is inherently self-aligning, a small amount of eccentricity may occur, arising from either the specimen being slightly curved or the epoxy bonding being slightly off-center in the pistons. Procedures to correct for this source of error exist and have been described by several investigators [9–12]. Where required, such corrections have been applied to all tensile data used in estimating fracture toughness discussed in this report. Typically, these corrections are in the 3–5% range and in no case exceeded 10%. The stress is related to the pressure and test geometry by the following equation:

$$\sigma = \sigma_{\text{NOM}} + \Delta\sigma = (A - A_s)/A_s \cdot P + \Delta\sigma, \quad (1)$$

where  $\sigma_{\text{NOM}}$  is the nominal fracture stress,  $\Delta\sigma$  is the correction for eccentricity which is equal to  $\sigma_{\text{NOM}} \times f$  (fracture origin location, specimen eccentricity and diameter),  $A$  is the cross-sectional area of the piston,  $A_s$  is the cross-sectional area of the specimen, and  $P$  is the pressure at failure, respectively.

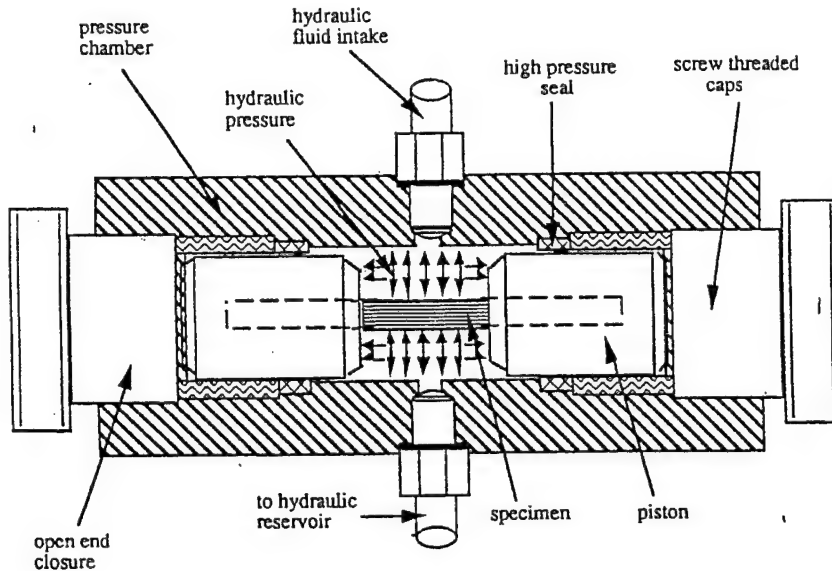
SEPB tests [13] were performed to measure the fracture toughness of materials from the same lots of materials used for tensile testing. At least six valid [14] SEPB tests and more usually 10–14 valid tests were performed for each material using 3- × 4- × 25-mm beams. Precracking was accomplished by indenting the 3-mm face of each specimen with a Vickers diamond indenter (with the diagonals parallel to the edges of the beam) and loaded in a double anvil configuration to

---

\* ARALDITE AV 118, Ciba Geigy Corp., Madison Heights, MI 48071.

† ASCERA Hydraulic Tensile Tester, Robertsfors, Sweden.

## UNIAXIAL TEST



$$\sigma = \sigma_{\text{NOM}} + \Delta\sigma = (A - A_S) / A_S \times P + \Delta\sigma,$$

$$\text{where } \Delta\sigma = f(r, e, d) \times \sigma_{\text{NOM}}$$

**Figure 1. Hydraulic Pressure Chamber With Specimen-Piston Assembly.**

“pop-in” a straight crack [15]. “Pop-in” and fracture toughness measurements were carried out on Instron model 8502 and 4201 testing machines,\* respectively. Detailed descriptions of the SEPB test procedure are available in Bar-On et al. and Quinn et al. [15, 16].

Fractographic examination of the fracture surfaces of the tensile bars was carried out in a JEOL 840A SEM.† Fracture surfaces were cleaned with acetone and coated with Au-Pd or carbon prior to SEM examination. Fractographic analysis of the tensile failures are conducted prior to carrying out  $K_{\text{IC}}$  measurements by SEPB. This avoids any subconscious bias in the measurement of the critical flaw size for the  $K_{\text{IC}}$  estimate.

\* Instron Corp., Canton, MA 02021.

† JEOL USA, Inc., Peabody, MA 01961.

The materials data and their source used in this work are listed in Table 1. The methodology used to estimate fracture toughness from the fractography of failed uniaxial tensile bars is presented in the following section.

**Table 1. Materials and Property Data Used in This Study**

Material	Source	$T - \sigma_{\text{CHAR}}$	m	AGS <sup>a</sup> ( $\mu\text{m}$ )	Reference
HP TiB <sub>2</sub>	Cercom	275	14.9	15	This study
HP AlN	Dow	234	12.7	1.9	Katz et al.
HP 50AlN/50SiC	Dow	361	26.4	0.5	Katz et al.
HP 75AlN/25SiC	Dow	371	9.9	2 <sup>b</sup> and 5 <sup>c</sup>	Katz et al.
HP SiC Pad B	Cercom	304 <sup>d</sup>	9.6 <sup>d</sup>	4.0	Cho, Katz, and Bar-On
HP SiC Pad N	Cercom	347 <sup>d</sup>	9.6 <sup>d</sup>	4.0	Cho, Katz, and Bar-On

Note: HP = hot pressed;  $T - \sigma_{\text{CHAR}}$  = tensile characteristic strength; m = Weibull Modulus; and AGS = average grain size.

<sup>a</sup> Based on the company product literature.

<sup>b</sup> AGS of AlN.

<sup>c</sup> AGS of SiC.

<sup>d</sup> Combined test data obtained from specimens machined by two vendors.

### 3. Criteria for Estimation of $K_{\text{IC}}$ by Fractographic Analysis

Only a fraction of the fracture surfaces resulting from uniaxial tensile failures are suitable for estimating  $K_{\text{IC}}$ . Not all samples have an obvious failure origin; this is often the case for samples failing from surface "defects." In a previous report [6], the authors and their coworkers defined a set of empirical conditions, which restrict those samples to be used for  $K_{\text{IC}}$  estimation. Later, this report will show that, in fact, these restrictions are necessary for close estimation of  $K_{\text{IC}}$  (within approximately 10%), and if they are relaxed, the difference between the estimated values and the values measured by SEPB tests increases significantly. The criteria for selecting samples for fracture toughness estimates are:

- (1) The failure must be from an internal flaw.
- (2) Fracture origins must exhibit fully developed “mirror,” mist, and hackle regions.
- (3) The mirror has to be “essentially” circular (samples with ellipsoidal mirrors are occasionally encountered and are not used).
- (4) The mirror, mist, and hackle regions must be close to normal to the specimen axis. (This ensures that the onset of unstable fracture occurred under a pure uniaxial stress field.)
- (5) The largest linear dimension of the failure initiating flaw at the center of the mirror is used as the crack length in the  $K_{IC}$  calculation.

The toughness,  $K_{IC}$ , is calculated using the Sneddon closed-form solution for a penny-shaped crack [17]:

$$K_{IC} = 2 \sigma_c (a_c/\pi)^{1/2}, \quad (2)$$

where  $\sigma_c$  is the failure stress and  $a_c$  is one-half the principal flaw dimension. It is worth noting that criteria (1) and (4) address issues raised by Rice with regard to improving the accuracy of fractographic estimation of  $K_{IC}$  [2].

Figure 2 shows a specimen of AlN which exhibits a well-defined mirror, mist, and hackle, as well as a circular mirror. This typifies an acceptable specimen for  $K_{IC}$  estimation. Figure 3 shows a specimen of an AlN-SiC solid solution that has an elliptical mirror and is therefore unacceptable for use in estimation of  $K_{IC}$ . Figure 4 shows a specimen of TiB<sub>2</sub> which has what we refer to as a “pseudo mirror.” In this case, there is a circular area which suggests a mirror, but upon close examination, it can be seen that no mirror, mist, and hackle regions are truly present, only mist and hackle. It will be shown later that such fracture origins are associated with significant underestimation of  $K_{IC}$ .

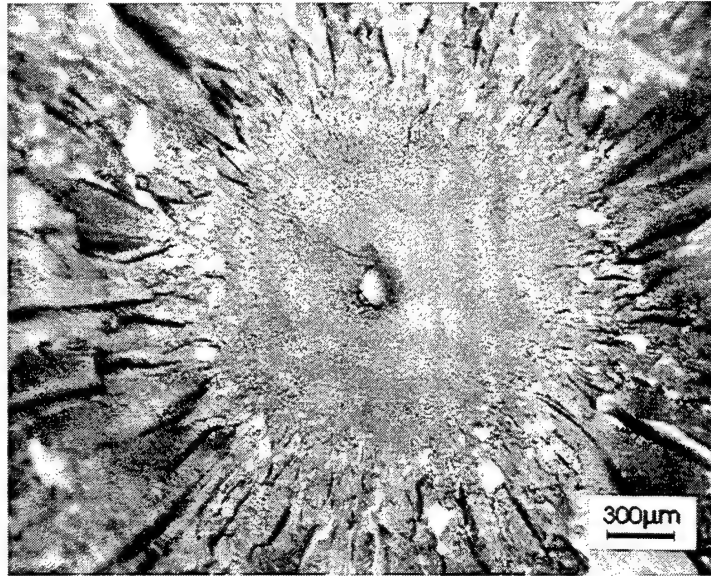


**Figure 2. Circular Fracture Mirror in AlN.**

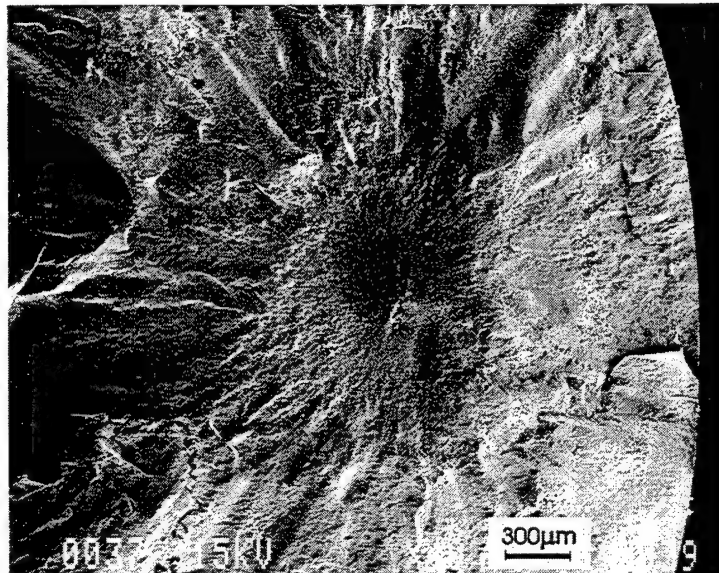


**Figure 3. Elliptical Fracture Mirror in AlN-SiC Solid Solution Unacceptable for Analysis.**



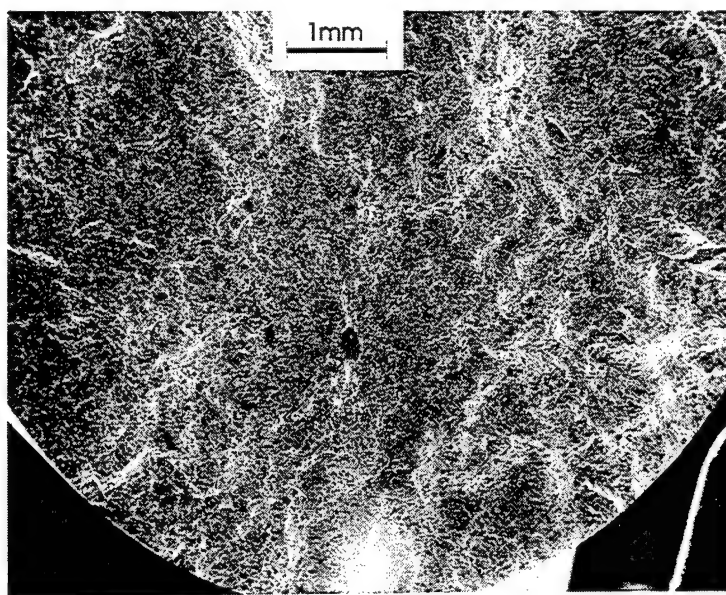


**Figure 4. "Pseudo" Mirror in  $\text{TiB}_2$  Shows Mist and Hackle But No Mirror.**

Whether or not a given material has a mirror associated with the fracture origin can be a function of the chemistry, phase content, and processing history. For example, we have examined the fracture origins in three different SiCs. A Dow experimental SiC\* did not exhibit a mirror or mist region. Cercom Pad B† material did exhibit mirror, mist, and hackle (Figure 5), whereas Cercom Pad N† material exhibited no mirror but only mist and hackle (Figure 6).

#### **4. Estimation of $K_{IC}$**

Using the previous criteria, estimates of  $K_{IC}$  were made for the six materials listed in Table 1. SEPB  $K_{IC}$  measurements were also made on these six materials. Figure 7 presents a plot of the fractographic estimations vs. the measured SEPB values. Very good agreement between the

---

\* Dow Chemical Co., Midland, MI 48674.

† Cercom, Inc., Vista, CA 92083.



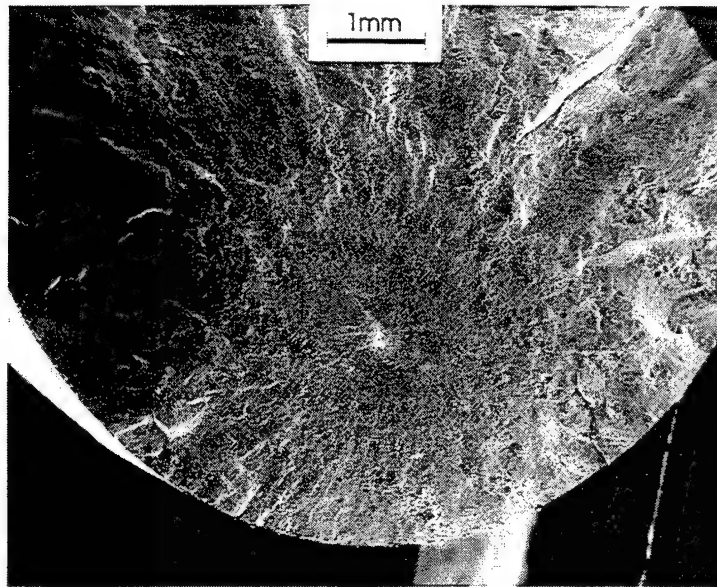


**Figure 5. SiC Pad B Shows Mirror, Mist, and Hackle.**

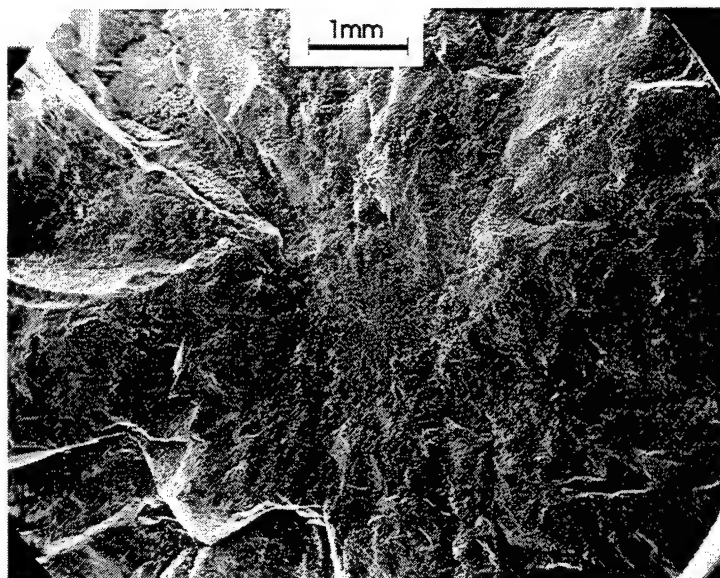


**Figure 6. SiC Pad N Shows Only Mist and Hackle.**

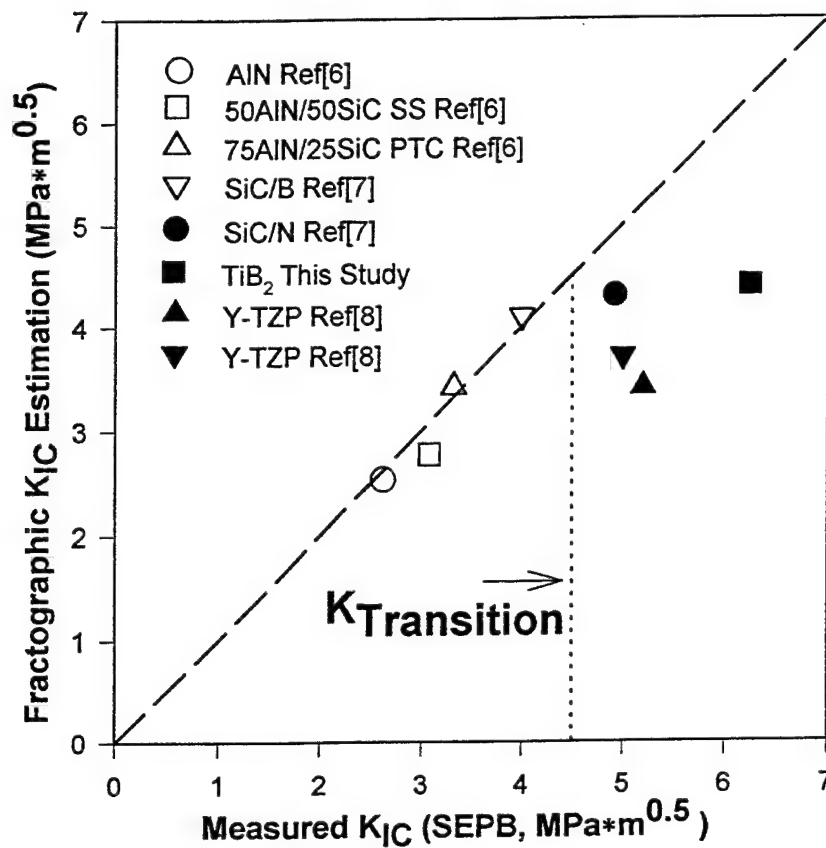


**Figure 7. Fracture toughness comparison between fractographic estimates and SEPB measurements.**

estimated and measured values is obtained for  $K_{IC}$  values determined by SEPB of less than  $\sim 4.5 \text{ MPa}\sqrt{\text{m}}$ . Around this value, the estimates of  $K_{IC}$  by fractography begin to substantially underestimate the measured values.

This behavior led us to reexamine the fracture surfaces and calculations that we had used in estimating  $K_{IC}$ . Upon reexamination, it became apparent that we had “relaxed” criterion (2) and used specimens exhibiting “pseudo mirrors.” This clearly emphasized the importance of rigorously applying all of the empirical criteria listed previously, in estimating  $K_{IC}$  using fractography. Rationalizing the observed behavior will be the concern of the balance of the report.

## 5. Potential Sources of Discrepancy Between Estimated and Measured $K_{IC}$ at "High" $K_{IC}$

While the tensile test technique of Oishi et al. [8] differed substantially from those used by the present authors and their colleagues, the variation that they found in estimated and measured  $K_{IC}$  is similar to that observed by other investigators as one goes from "small" flaws to "large" flaws in Y-TZP. The increase in fracture toughness as the flaw size increases has been related to "micro R-curve behavior" [4]. Rice's data on estimation of  $K_{IC}$  as a function of flaw size for TZP and ZTA materials also show evidence of "micro R-curve behavior" [2]. It is reasonable that the difference in fracture toughness encountered between large artificially induced flaws, such as in an SEPB test, and the small naturally occurring flaws used in fractographic estimation would be very sensitive to R-curve behavior. Swab and Quinn [4] point out that one cause of observing critical flaws significantly smaller than those predicted from macroscopic fracture toughness tests is the presence of R-curve behavior. As shown in Table 2, the range of flaws measured on  $TiB_2$  tensile fracture surfaces is significantly smaller than the average flaw anticipated using the average strength and measured fracture toughness. By contrast, in the case of AlN and AlN/SiC solid solution, the observed flaw sizes bracket the predicted flaw size, as anticipated. The presence of behavior consistent with a given mechanism, however, only means that the mechanism is plausible. Other mechanisms may, in fact, be responsible for the observed behavior.

**Table 2. Anticipated vs. Observed Flaw Size**

	AlN	50 AlN/50 SiC	$TiB_2$
Average $\sigma_c$	230 MPa	360 MPa	280 MPa
Average $K_{IC}$	2.62 MPa $\sqrt{m}$	3.08 MPa $\sqrt{m}$	6.25 MPa $\sqrt{m}$ calculated
Average $a_0$	~100 $\mu m$	~57 $\mu m$	~390 $\mu m$
Observed ranges of $a_0$	42–135 $\mu m$	5–200 $\mu m$	170–280 $\mu m$

Note:  $\sigma_c$  = fracture stress;  $a_0$  = flaw size.

An alternative mechanism may be subcritical crack growth without R-curve behavior. Normally, one associates subcritical crack growth with slow crack growth at high temperatures or in the presence of water or other reactive environment. Neither situation prevailed in the tensile testing reported in this work. All tests were at room temperature and since the fracture origins were well in the volume, not near the surface, no reaction with the hydraulic pressurization fluid was possible. Therefore, the most plausible explanation for the existence of subcritical crack growth, in  $\text{TiB}_2$ , is R-curve behavior as described by Bennison and Lawn [18]. To settle the issue, an investigation of R-curve behavior in  $\text{TiB}_2$  should be undertaken.

## 6. The Fracture Initiating Flaw vs. the Critical Flaw

In ceramic materials that exhibit subcritical crack growth, whether associated with R-curve behavior or some other cause, the fracture initiating flaw will not be the critical flaw for fracture mechanics purposes. An interesting example of this was encountered in one  $\text{TiB}_2$  specimen examined in this study. The fracture origin of the specimen shown in Figure 4 is detailed at increasing magnifications. Figure 8a shows the large grain at the center of the "pseudo-mirror." Figure 8b shows that this grain itself has a true fracture mirror with a small ( $\sim 20 \mu\text{m}$ ) particle at the center of the mirror. This inclusion showed traces of W, Co, Fe, and Ni (by EDXS), which are all consistent with a fragment of WC grinding media. It is probable that this inclusion was the initiating flaw, but it is much too small to be the critical flaw.

Similarly, the large grain is too small to be the critical flaw predicted by fracture mechanics based on the conventional large flaw toughness measurement. Even the various ellipses that one can imagine seeing, linking large grains surrounding the very large grain in Figure 8a, are not large enough to be the critical flaw. It is evident that care should be taken not to use the terms "fracture initiating flaw" and "critical flaw" interchangeably. They may or may not be equal.

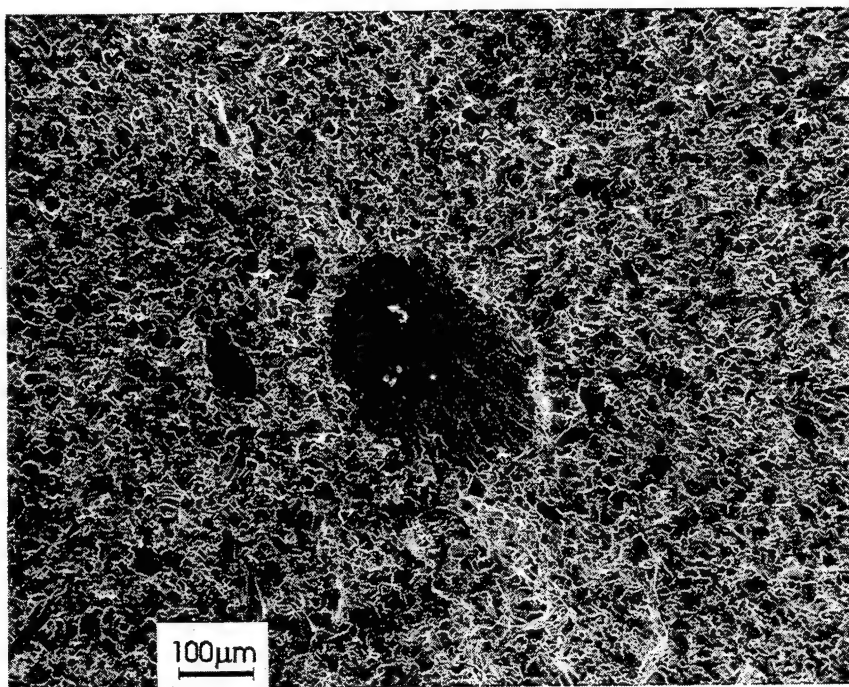


**Figure 8a. Large Grain at Origin of Fracture in TiB<sub>2</sub> Specimen.**

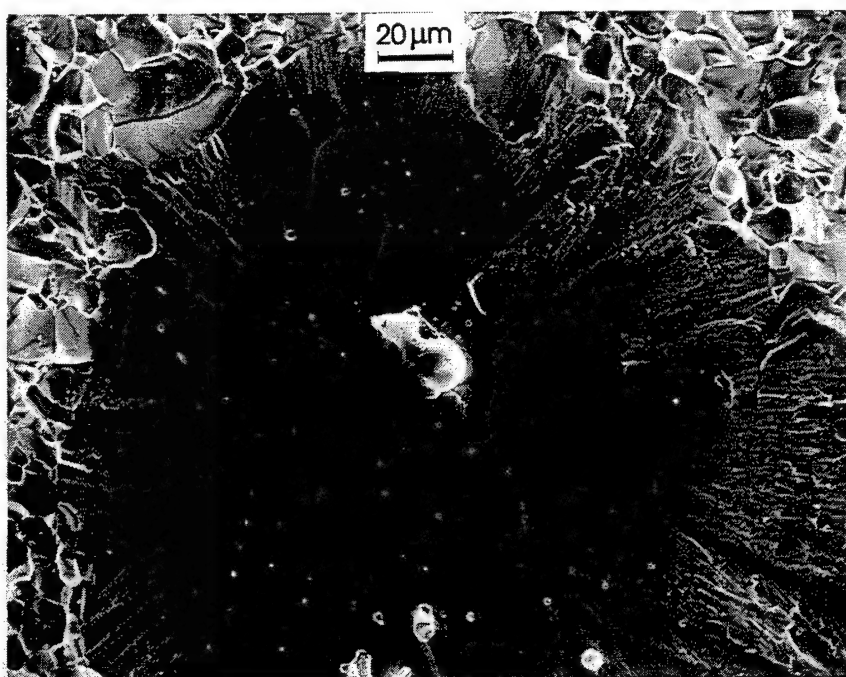


**Figure 8b. Particle in Large Grain at Origin of Fracture in TiB<sub>2</sub> Specimen.**

## 7. Summary

We have shown that if the empirical criteria presented in this report are applied, excellent correlation between fractographically estimated and measured  $K_{IC}$  can be attained. It is especially critical in applying these criteria to be certain that a true fracture mirror is present. By implication, if the estimated  $K_{IC}$  lies on the curve in Figure 7, it can be taken as evidence of a lack of R-curve behavior. Conversely, if the estimated  $K_{IC}$  lies substantially below the curve in Figure 7, R-curve behavior may be present. It has also been shown that for "tough" ceramics, the terms "failure initiating" and "critical flaw" are not synonymous.

## 8. References

1. Mecholsky, J. J., Jr., S. W. Freiman, and R. W. Rice. "Fracture Surface Analysis of Ceramics." *J. Mat. Sci.*, vol. 11, pp. 1310-19, 1990.
2. Rice, R. W. "Fractographic Determination of  $K_{IC}$  and Effects of Microstructural Stresses in Ceramics." *Fractography of Glasses and Ceramics II*, edited by V. D. Frechette and J. R. Varner, American Ceramic Society, pp. 509-545, 1991.
3. U.S. Department of Defense. *Fractography and Characterization of Fracture Origins in Advanced Structural Ceramics*. Military Handbook, MIL-HDBK-790, 1 July 1992.
4. Swab, J. J., and G. Quinn. "Fractography of Advanced Structural Ceramics: Results From the VAMAS Round Robin Exercise." ARL-TR-656, U.S. Army Research Laboratory, Aberdeen Proving Ground, MD, December 1994.
5. Baratta, F. I., G. W. Driscoll, and R. N. Katz. "The Use of Fracture Mechanics and Fractography to Define Surface Finish Requirements for  $Si_3N_4$ ." *Ceramics for High Performance Applications*, edited by J. J. Burke, A. E. Gorum, and R. N. Katz, MA: Brook Hill Publication, pp. 445-476, 1974.
6. Katz, R. N., S. Grendahl, K. Cho, I. Bar-On, and W. Rafaniello. "Fracture Toughness of Ceramics in the AlN-SiC System." *Ceram. Eng. Sci. Proc.*, vol. 15, no. 5, pp. 877-884, 1994.
7. Cho, K., R. N. Katz, and I. Bar-On. "Strength and Fracture Toughness of Hot Pressed SiC Materials." *Ceram. Eng. Sci. Proc.*, vol. 16, no. 4, pp. 105-112, 1995.
8. Oishi, M., Y. Matsuda, K. Noguchi, and T. Masaki. "Evaluation of Tensile Strength and Fracture Toughness of Y-Stabilized Zirconia Polycrystals With Fracture Surface Analysis." *J. Am. Ceram. Soc.*, vol. 78, no. 5, pp. 1212-16, 1995.
9. Nilson, J., and B. Mattson. "A New Tensile Test Method for Ceramic Materials." *Proceedings of 2nd International Symposium on Ceramic Materials and Components for Engines*, edited by W. Bunk and H. Hausner, Deutsche Keramische Gesellschaft, Wiesbaden, 1986.
10. Lucas, H. P. "Direct Tensile Testing of Brittle Materials." Master Thesis, Worcester Polytechnic Institute, Worcester, MA, 1991.
11. Tautanjii, H. A. "The Development of a Cementitious Composites Test Technique and Its Application to Carbon Fiber Reinforced Cementitious Composites." Ph.D. Thesis, Worcester Polytechnic Institute, Worcester, MA, 1992.

12. Hermanson, L., J. Adlerborn, and M. Burstrom. "Tensile Testing of Ceramic Materials - A New Approach." *High Tech Ceramics*, edited by P. Vicenzini, Amsterdam: Elsevier Science Publication, pp. 1161-68, 1987.
13. Nose, T., and T. Fujii. "Evaluation of Fracture Toughness for Ceramics Materials by a Single-Edge Precracked-Beam Method." *J. Am. Ceram. Soc.*, vol. 71, no. 5, pp. 328-333, 1988.
14. Army Society for Testing and Materials. "Standard Test Method for Plane-Strain Fracture Toughness of Metallic Materials." ASTM STD E-399, Annual Book of ASTM Standards, vol. 03.01, pp. 487-511, 1989.
15. Bar-On, I., J. Beals, G. Leatherman, and C. Murray. Fracture Toughness of Ceramic Precracked Bend Bars." *J. Am. Ceram. Soc.*, vol. 73, no. 8, pp. 2519-22, 1990.
16. Quinn, G. D., J. Salem, I. Bar-On, K. Cho, M. Foley, and H. Fang. "Fracture Toughness of Advanced Ceramics at Room Temperature." *J. Res. Natl. Inst. Stand. Technol.*, vol. 97, no. 5, pp. 579-607, 1992.
17. Sneddon, I. N. "The Stress Distribution in the Neighborhood of a Crack in an Elastic Solid." *Proc. Royal Soc. Ser. A*, vol. 187, pp. 229-260, 1949.
18. Bennison, S. J., and R. R. Lawn. "Origin Tolerance in Ceramics With Rising Crack Resistance Characteristics." *J. Mat. Sci.*, vol. 24, pp. 3169-75, 1989.



NO. OF  
COPIES ORGANIZATION

2 DEFENSE TECHNICAL  
INFORMATION CENTER  
DTIC DDA  
8725 JOHN J KINGMAN RD  
STE 0944  
FT BELVOIR VA 22060-6218

1 HQDA  
DAMO FDQ  
DENNIS SCHMIDT  
400 ARMY PENTAGON  
WASHINGTON DC 20310-0460

1 CECOM  
SP & TRRSTRL COMMCTN DIV  
AMSEL RD ST MC M  
H SOICHER  
FT MONMOUTH NJ 07703-5203

1 PRIN DPTY FOR TCHNLGY HQ  
US ARMY MATCOM  
AMCDCG T  
M FISETTE  
5001 EISENHOWER AVE  
ALEXANDRIA VA 22333-0001

1 PRIN DPTY FOR ACQUSTN HQS  
US ARMY MATCOM  
AMCDCG A  
D ADAMS  
5001 EISENHOWER AVE  
ALEXANDRIA VA 22333-0001

1 DPTY CG FOR RDE HQS  
US ARMY MATCOM  
AMCRD  
BG BEAUCHAMP  
5001 EISENHOWER AVE  
ALEXANDRIA VA 22333-0001

1 ASST DPTY CG FOR RDE HQS  
US ARMY MATCOM  
AMCRD  
COL S MANESS  
5001 EISENHOWER AVE  
ALEXANDRIA VA 22333-0001

NO. OF  
COPIES ORGANIZATION

1 DPTY ASSIST SCY FOR R&T  
SARD TT F MILTON  
THE PENTAGON RM 3E479  
WASHINGTON DC 20310-0103

1 DPTY ASSIST SCY FOR R&T  
SARD TT D CHAIT  
THE PENTAGON  
WASHINGTON DC 20310-0103

1 DPTY ASSIST SCY FOR R&T  
SARD TT K KOMINOS  
THE PENTAGON  
WASHINGTON DC 20310-0103

1 DPTY ASSIST SCY FOR R&T  
SARD TT B REISMAN  
THE PENTAGON  
WASHINGTON DC 20310-0103

1 DPTY ASSIST SCY FOR R&T  
SARD TT T KILLION  
THE PENTAGON  
WASHINGTON DC 20310-0103

1 OSD  
OUSD(A&T)/ODDDR&E(R)  
J LUPO  
THE PENTAGON  
WASHINGTON DC 20301-7100

1 INST FOR ADVNCD TCHNLGY  
THE UNIV OF TEXAS AT AUSTIN  
PO BOX 202797  
AUSTIN TX 78720-2797

1 DUSD SPACE  
1E765 J G MCNEFF  
3900 DEFENSE PENTAGON  
WASHINGTON DC 20301-3900

1 USAASA  
MOAS AI W PARRON  
9325 GUNSTON RD STE N319  
FT BELVOIR VA 22060-5582

NO. OF  
COPIES ORGANIZATION

- 1 CECOM  
PM GPS COL S YOUNG  
FT MONMOUTH NJ 07703
- 1 GPS JOINT PROG OFC DIR  
COL J CLAY  
2435 VELA WAY STE 1613  
LOS ANGELES AFB CA 90245-5500
- 1 ELECTRONIC SYS DIV DIR  
CECOM RDEC  
J NIEMELA  
FT MONMOUTH NJ 07703
- 3 DARPA  
L STOTTS  
J PENNELLA  
B KASPAR  
3701 N FAIRFAX DR  
ARLINGTON VA 22203-1714
- 1 SPCL ASST TO WING CMNDR  
50SW/CCX  
CAPT P H BERNSTEIN  
300 O'MALLEY AVE STE 20  
FALCON AFB CO 80912-3020
- 1 USAF SMC/CED  
DMA/JPO  
M ISON  
2435 VELA WAY STE 1613  
LOS ANGELES AFB CA 90245-5500
- 1 US MILITARY ACADEMY  
MATH SCI CTR OF EXCELLENCE  
DEPT OF MATHEMATICAL SCI  
MDN A MAJ DON ENGEN  
THAYER HALL  
WEST POINT NY 10996-1786
- 1 DIRECTOR  
US ARMY RESEARCH LAB  
AMSRL CS AL TP  
2800 POWDER MILL RD  
ADELPHI MD 20783-1145

NO. OF  
COPIES ORGANIZATION

- 1 DIRECTOR  
US ARMY RESEARCH LAB  
AMSRL CS AL TA  
2800 POWDER MILL RD  
ADELPHI MD 20783-1145

- 3 DIRECTOR  
US ARMY RESEARCH LAB  
AMSRL CI LL  
2800 POWDER MILL RD  
ADELPHI MD 20783-1145

ABERDEEN PROVING GROUND

- 2 DIR USARL  
AMSRL CI LP (305)

<u>NO. OF COPIES</u>	<u>ORGANIZATION</u>
1	COMMANDER US ARMY RESEARCH OFC INFO PROCESSING OFC PO BOX 12211 RESEARCH TRIANGLE PARK NC 27709-2211
1	COMMANDER USAMC AMCSCI 5001 EISENHOWER AVE ALEXANDRIA VA 22333
2	COMMANDER US ARMY ARDEC TECH LIB DR K WILLISON PICATINNY ARSENAL NJ 07806-5000
1	COMMANDER US ARMY TACOM AMSTA TSL TECH LIB WARREN MI 48297-5000
1	NATL INST OF STANDARDS & TECH GEORGE QUINN CERAMICS DIV BLDG 223 A326 GAITHERSBURG MD 02899
14	WORCESTER POLYTECH INST DR R BIEDERMAN DR R SISSON DR ISA BAR-ON DR MARINA PASCUCI DR R NATHAN KATZ (10 CPS) 100 INSTITUTE RD WORCESTER MA 01609
1	MIAC/CINDAS PURDUE UNIVERSITY 2595 YEAGER RD WEST LAFAYETTE IN 47905

<u>NO. OF COPIES</u>	<u>ORGANIZATION</u>
3	MATERIALS MODIFICATION INC DR T S SUDARSHAN DR SANG YOO RESHINA KUMAR 2929-P1 ESKRIDGE RD FAIRFAX VA 22031
1	CERCOM INC DR JAMES SHIH 1960 WATSON WAY VISTA CA 92083
10	MR FRANCIS BARATTA 138 RIDGE ST ARLINGTON MA 02174-1737
	<u>ABERDEEN PROVING GROUND</u>
27	DIR USARL AMSRL WM M DR DENNIS VIECHNCKI AMSRL WM MC DR THOMAS V HYNES DR JOSEPH WELLS JEFFREY J SWAB GARY A GILDE DR JERRY LASALVIA AMSRL WM MD ROBERT DOWDING KYU CHO (20 CPS)
1	DIR USAMSAA AMXSYP MP

INTENTIONALLY LEFT BLANK.

REPORT DOCUMENTATION PAGE			Form Approved OMB No. 0704-0188	
<small>Public reporting burden for this collection of information is estimated to average 1 hour per response, including the time for reviewing instructions, searching existing data sources, gathering and maintaining the data needed, and completing and reviewing the collection of information. Send comments regarding this burden estimate or any other aspect of this collection of information, including suggestions for reducing this burden, to Washington Headquarters Services, Directorate for Information Operations and Reports, 1215 Jefferson Davis Highway, Suite 1204, Arlington, VA 22202-4302, and to the Office of Management and Budget, Paperwork Reduction Project (0704-0188), Washington, DC 20503.</small>				
1. AGENCY USE ONLY (Leave blank)	2. REPORT DATE June 1997	3. REPORT TYPE AND DATES COVERED Final, Oct 94 - Sep 96		
4. TITLE AND SUBTITLE  Fracture Toughness Estimation From Ceramic Tensile Specimens by Fractographic Analysis		5. FUNDING NUMBERS  44LAL 552LBA		
6. AUTHOR(S)  R. Nathan Katz* and Kyu Cho				
7. PERFORMING ORGANIZATION NAME(S) AND ADDRESS(ES)  U.S. Army Research Laboratory ATTN: AMSRL-WM-MD Aberdeen Proving Ground, MD 21005-5069		8. PERFORMING ORGANIZATION REPORT NUMBER  ARL-TR-1405		
9. SPONSORING/MONITORING AGENCY NAMES(S) AND ADDRESS(ES)		10. SPONSORING/MONITORING AGENCY REPORT NUMBER		
11. SUPPLEMENTARY NOTES * Recently retired from the U.S. Army Research Laboratory and currently at the Mechanical Engineering Department, Worcester Polytechnic Institute, Worcester, MA 01609.				
12a. DISTRIBUTION/AVAILABILITY STATEMENT  Approved for public release; distribution is unlimited.		12b. DISTRIBUTION CODE		
13. ABSTRACT (Maximum 200 words)  Empirical criteria are presented for selection of uniaxial tensile failure origins that will yield valid fracture toughness estimations. Using these criteria, estimations of fracture toughness based on fractography of an AIN, two SiCs, a AIN-SiC solid solution and a particulate composite, and a TiB <sub>2</sub> were performed. Comparison of the fracture toughness values estimated from fractography with fracture toughness measured by the single-edge precracked beam (SEPB) method will be shown. Close agreement is observed between estimates made from fractographic analysis and measurements made on specimens with large artificially induced flaws if the fracture toughness is 4 MPa√m or below. For materials in which the SEPB fracture toughness is greater than about 4.8 MPa√m, estimates by fractographic analysis significantly underestimate the SEPB fracture toughness. In attempting to rationalize this discrepancy, the importance of rigorously applying the empirical criteria was reemphasized.				
14. SUBJECT TERMS  fracture toughness estimation, tensile, fractograph			15. NUMBER OF PAGES 25	
			16. PRICE CODE	
17. SECURITY CLASSIFICATION OF REPORT UNCLASSIFIED	18. SECURITY CLASSIFICATION OF THIS PAGE UNCLASSIFIED	19. SECURITY CLASSIFICATION OF ABSTRACT UNCLASSIFIED	20. LIMITATION OF ABSTRACT UL	

INTENTIONALLY LEFT BLANK.

## USER EVALUATION SHEET/CHANGE OF ADDRESS

This Laboratory undertakes a continuing effort to improve the quality of the reports it publishes. Your comments/answers to the items/questions below will aid us in our efforts.

1. ARL Report Number/Author ARL-TR-1405 (Katz) Date of Report June 1997

2. Date Report Received \_\_\_\_\_

3. Does this report satisfy a need? (Comment on purpose, related project, or other area of interest for which the report will be used.) \_\_\_\_\_  
\_\_\_\_\_  
\_\_\_\_\_

4. Specifically, how is the report being used? (Information source, design data, procedure, source of ideas, etc.) \_\_\_\_\_  
\_\_\_\_\_  
\_\_\_\_\_

5. Has the information in this report led to any quantitative savings as far as man-hours or dollars saved, operating costs avoided, or efficiencies achieved, etc? If so, please elaborate. \_\_\_\_\_  
\_\_\_\_\_  
\_\_\_\_\_

6. General Comments. What do you think should be changed to improve future reports? (Indicate changes to organization, technical content, format, etc.) \_\_\_\_\_  
\_\_\_\_\_  
\_\_\_\_\_  
\_\_\_\_\_

CURRENT  
ADDRESS

\_\_\_\_\_  
Organization

\_\_\_\_\_  
Name

\_\_\_\_\_  
E-mail Name

\_\_\_\_\_  
Street or P.O. Box No.

\_\_\_\_\_  
City, State, Zip Code

7. If indicating a Change of Address or Address Correction, please provide the Current or Correct address above and the Old or Incorrect address below.

OLD  
ADDRESS

\_\_\_\_\_  
Organization

\_\_\_\_\_  
Name

\_\_\_\_\_  
Street or P.O. Box No.

\_\_\_\_\_  
City, State, Zip Code

(Remove this sheet, fold as indicated, tape closed, and mail.)  
(DO NOT STAPLE)

---

DEPARTMENT OF THE ARMY

OFFICIAL BUSINESS

**BUSINESS REPLY MAIL**  
FIRST CLASS PERMIT NO 0001,APG,MD

POSTAGE WILL BE PAID BY ADDRESSEE

DIRECTOR  
US ARMY RESEARCH LABORATORY  
ATTN AMSRL WM MD  
ABERDEEN PROVING GROUND MD 21005-5066



NO POSTAGE  
NECESSARY  
IF MAILED  
IN THE  
UNITED STATES

